Int J Adv Manuf Technol (2016) 83:505–517
DOI 10.1007/s00170-015-7575-3

ORIGINAL ARTICLE

Drilling of film cooling holes by a EDM/ECM in situ combined process using internal and side flushing of tubular electrode

Yan Zhang[1] · **Zhengyang Xu**[1] · **Di Zhu**[1] · **Ningsong Qu**[1] · **Yun Zhu**[1]

Received: 28 February 2015 / Accepted: 5 July 2015 / Published online: 25 July 2015
© Springer-Verlag London 2015

Abstract To allow very high turbine inlet gas temperatures, film cooling holes are widely applied in gas turbine engines. Owing to the requirements of high machining efficiency and surface quality, the fabrication of film cooling holes in difficult-to-machine materials is extremely difficult. A tubular electrode electro-discharge high-speed drilling/electrochemical machining (ECM) in situ combined process has been proposed for this task. In this approach, electro-discharge machining (EDM) is efficiently employed to form the holes, following which the recast layer thereby generated is removed from the machined surface by electrochemical dissolution. In this study, a tubular electrode and a specially designed flushing device are used, with internal and side flushing being performed at the same time so that EDM and ECM can be combined in situ. The performance of the technique is investigated on a nickel-based superalloy. To achieve the best performance, the ideal values of EDM parameters (peak current, pulse duration, and pulse interval) are determined. The ECM is employed to remove the rough surface produced by the EDM. Compared with EDM alone, it is found that the EDM/ECM in situ combined process improves the surface quality of the holes and removes the recast layer. It is confirmed that the combined process is suitable for producing film cooling holes without a recast layer.

Keywords Electro-discharge machining · Electrochemical machining · EDM/ECM combined process · Nickel-based superalloy · Film cooling hole · Recast layer

✉ Zhengyang Xu
xuzhy@nuaa.edu.cn

Yan Zhang
zhangyanzy@nuaa.edu.cn

Di Zhu
dzhu@nuaa.edu.cn

Ningsong Qu
nsqu@nuaa.edu.cn

Yun Zhu
zhuyun_youxiang@163.com

[1] College of Mechanical and Electrical Engineering, Nanjing University of Aeronautics & Astronautics, 29 Yudao St., Nanjing 210016, China

1 Introduction

In the aerospace industry, there is an increasingly wide range of applications for small-size, high-precision, and high-quality products and components in which large numbers of microscopic and small holes are drilled [1]. For example, in the case of aero-engines, film cooling allows gas turbines to operate at higher turbine firing temperatures and efficiencies and with a longer service life [2]. The technology necessary for this relies upon the use of large numbers of very small film cooling holes, distributed in a variety of ways on the surface of the relevant engine component (e.g., a turbine blade or vane). However, such components are made from high-strength, high-hardness, and difficult-to-machine materials, and therefore it has proved difficult to use conventional processes to machine the holes [3]. Hence, attention has increasingly been focused on nontraditional processes for producing film cooling holes with high efficiency and surface quality.

Electro-discharge machining (EDM) has become the predominant processing technology for film cooling holes, owing to its unique advantages [4, 5]. As an

electro-thermal technique, EDM can be used to machine any conductive material, including superalloys and other difficult-to-machine materials, effectively and accurately [6–8]. In addition, because there is no direct contact between workpiece and tool electrode, EDM does not produce mechanical stress and is suitable for the fabrication of microstructures [9, 10]. In spite of these advantages, however, EDM, owing to its thermal processing mechanism, suffers from the significant drawback that the processed surface is covered with thermally damaged layers composed of a recast layer and heat-affected zones [11, 12]. In particular, voids, cracks, and thermal stress within the recast layer decrease the material's resistance to fatigue and corrosion [13], with detrimental effects on the component's mechanical properties, particularly under extreme working conditions [14]. Therefore, it is desirable that a method be found for machining film cooling holes without recast layers, which is not possible with the use of EDM alone.

There have been a number of investigations of machining of surfaces using EDM in combination with other techniques. McGeough et al. [15] performed a theoretical and experimental investigation to improve surface quality using a hybrid machine combining EDM and electrochemical machining (ECM). Kurita and Hattori [16] investigated the use of ECM lapping to obtain a smooth surface after EDM shaping. Chung et al. [17] focusing on a micro-EDM hole surface finishing process based on electrochemical dissolution using deionized water, studied the effects of finishing conditions on surface roughness. Ramasawmy et al. [18] investigated the effects of electrochemical polishing parameters on EDM surfaces. Zeng et al. [19] performed an experimental study of micro-EDM/micro-ECM combined milling for three-dimensional micro-structures and found that EDM surface defects could be completely removed by micro-ECM milling.

Compared with the preceding examples emphasizing surface finishing, in this study, a greater importance is attached to efficiency and the absence of a recast layer. Previous studies have shown that ECM, owing to benefits such as the absence of residual stress, cracks, and heat-affected zones [20, 21], is an effective method for improving the quality of surfaces generated by EDM [22, 23]. Hence, for film cooling holes, a hybrid process combining EDM and ECM is promising, since during the combined machining, the benefits of these two processes are appropriately employed and defects are mitigated [24, 25]. In previous research, the primary focus has been on micrometer-scale structures, using fine cylindrical electrodes [26], whereas this study aims to machine film cooling holes without recast layers using a tubular electrode, especially for diameters greater than 0.5 mm. To achieve this aim, a combined EDM/ECM drilling system, using a specially designed electrolyte flow device, is employed. In this way, the combined processes can be performed sequentially on the same machine tool with the same tool electrode at the same workstation. Because the need for frequent substitution of fresh electrodes is thereby avoided, the efficiency is greatly improved. The principle of the combined machining principle is discussed, and the effects of the EDM and ECM parameters are identified.

2 Experimental details

2.1 Machine tool

The in situ combined EDM and ECM drilling processes were performed on a multi-process machine tool. A schematic diagram of the experimental equipment is shown in Fig. 1. The drilling system comprises a power supply

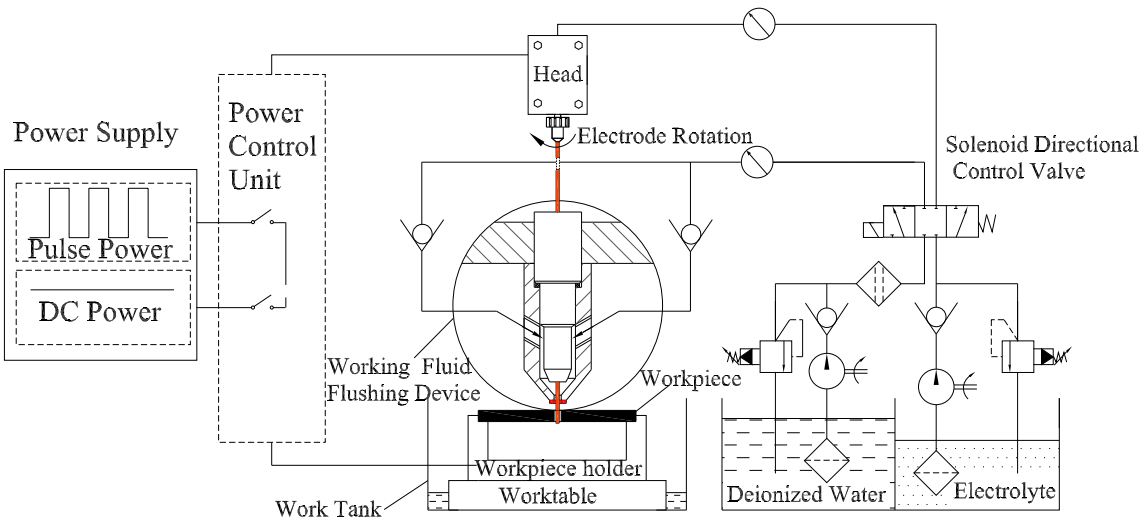

Fig 1 EDM and ECM in situ combined drilling system

unit, a dielectric circulation system, and a machining cell. The pulsed and DC power generated by the power supply unit can be sequentially applied between the tool electrode and the workpiece by the power control unit. The tubular electrode is fixed in the machining head and rotates with the spindle. In the dielectric circulation system, dielectric fluid is provided via the rotating tubular electrode to perform internal flushing. In addition, a special electrolyte flow device allows side flushing with electrolyte. With this design, the entire experiment can be carried out on the same machine tool with the same tool electrode without the need to re-clamp the electrode and workpiece.

2.2 Materials

Nickel-based superalloys are difficult to machine, but are extensively used in the aerospace industry because of their high rigidity and their good temperature, corrosion, and wear resistance. DZ125L, as a typical nickel-based direction detection coagulation superalloy, is widely used in turbine blades. In this study, experiments were conducted on a DZ125L superalloy plate of 3 mm thickness as the workpiece. In these experiments, all the holes have been drilled through the workpiece; thus, the depth of the machined holes could be considered as the thickness of the workpiece, 3 mm. The chemical composition of this workpiece is shown in Table 1. A brass tube was selected as the tool electrode.

2.3 Working fluid flushing device

The working fluid flushing device comprises an electrode guide, an electrolyte fairing, and a silicone seal gasket, as shown in Fig. 2. The electrolyte fairing is fixed on the electrode guide, such that a chamber is formed between them, and the tubular electrode passes through the interior of the device. During EDM, as the dielectric work fluid, the deionized water is supplied into the whole machining region from the inside of the tubular electrode, whereas during ECM, as the conducting medium, the electrolyte is flushed into the lateral machining gap through the fluid channel and downward along the side wall of the electrode guide and tubular electrode, as shown in the dotted line of Fig. 2. Using this device, internal and side flushing can be performed at the same time. It is thereby possible for EDM and ECM to be combined in situ to fabricate film cooling holes.

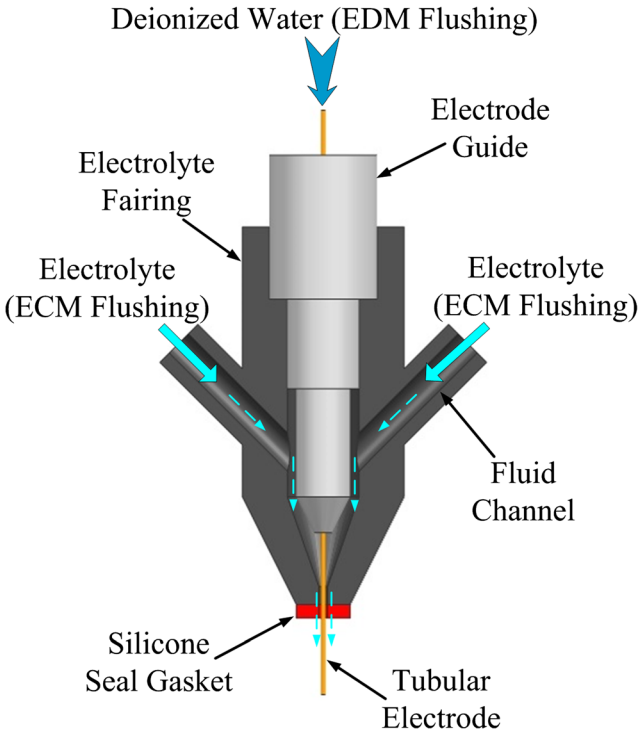

Fig 2 Working fluid flushing device

2.4 Principle and machining procedures

The principle of the EDM/ECM in situ combined processing is shown in Fig. 3. In this process, tubular electrode electro-discharge high-speed drilling and ECM are carried out in sequence. During EDM, the pulse generator is switched on, and the rotating tubular electrode moves toward the workpiece. Meanwhile, deionized water, as the dielectric fluid, is supplied to the machining region via the inside of the pipe electrode to enable high-speed EDM drilling. Following this, the tubular electrode stays at the same position, while the flushing device is fed toward the workpiece, with sodium nitrate solution flowing into the side gap. For a high material removal rate, DC power, instead of pulsed power, is applied to the inter-electrode gap, thereby enabling ECM to corrode and dissolve the recast layer formed by EDM. With this approach, tubular electrode electro-

Table 1 Chemical composition of DZ125L alloy (wt%)

Composition	C	Cr	Co	W	Mo	Ta	Al	Ni
	0.07–0.12	6.50–7.50	11.50–12.50	4.70–5.20	1.00–2.00	6.50–7.50	5.60–6.20	Remainder

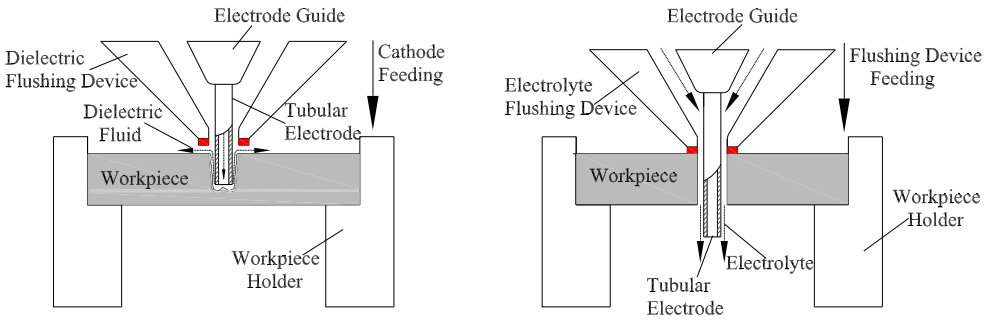

(a) EDM process (b) ECM process

Fig 3 **a**, **b** EDM/ECM in situ combined processing

discharge high-speed drilling and ECM are combined in situ to perform high-speed drilling without recast layers.

2.5 Machining conditions

The machining process is carried out in two stages, comprising EDM drilling and ECM finishing. In the first stage, a micro-hole is drilled by EDM with machining parameters as given in Table 2. In section 3.1, the different machining parameters for EDM have been tried. Deionized water with conductivity 0.55 μS/cm is used as the dielectric fluid for EDM. The effects of different machining parameters on machining performance in terms of material removal rate (MRR), average diameter, taper angle, and recast layer are examined. Among them, the difference value of the diameter is considered as the result of taper angle. Besides, the recast layer is examined metallographically. After cutting, polishing, and etching, cross sections of the recast layer were analyzed under a metallographic microscope. By means of OLYMPUS microscope GX71 which has the function of measurement, the thickness of recast layer could be measured. And the maximal thickness is examined as the results of recast layer, because only the maximal recast thicknesses produced in EDM are removed in the ECM process, can the surface which is free of recast layer be obtained finally. In the second stage, ECM, using a low-concentration electrolyte and the parameters listed in Table 3, is employed to finish the surface produced by EDM. The same tool electrode with a diameter of 500 μm is used in both stages, without being re-clamped. The final surfaces are compared with those produced by EDM alone.

Table 2 Experimental parameters for EDM

Machining parameter	Value
Pulse voltage	80 V
Pulse duration T_{on}	8, 12, 16, 20 μs
Pulse interval T_{off}	12, 24, 36, 48 μs
Peak current	8, 12, 16, 20 A
Diameter of electrode	500 μm
Working fluid	Deionized water
Fluid inlet pressure	4 MPa

3 Experimental results and discussion

3.1 Electrical discharge drilling process

In this section, there are two objectives to achieve. On one hand, the ideal machining performance including MRR, average diameter, taper angle, recast layer are expected to obtain. On the other hand, the effects of single parameter on all machining performances including the MRR, average diameter, taper angle, recast layer are also analyzed, respectively. It is expected that the regular pattern found and shown in this section could be used to guide the subsequent research.

3.1.1 Effects of peak current on machining performance

The machining results using various peak currents are plotted in Fig. 4. The other machining parameters are set at a pulse duration of 12 μs and pulse interval of 24 μs. The figure reveals that the MRR and the thickness of recast layer show an upward trend with increasing peak current. Additionally, with increasing peak current, the average diameter rises to 593.5 μm and then decreases, while the taper angle decreases and then increases, with the minimum taper angle being obtained at a peak current of 12 A. Through a compromise among

Table 3 Process parameters for ECM

Parameter	Value
Voltage	15, 30, 45 V
Machining time	15, 30, 45, 60 s
Diameter of electrode	500 μm
Working fluid	Sodium nitrate solution
Fluid inlet pressure	2 MPa

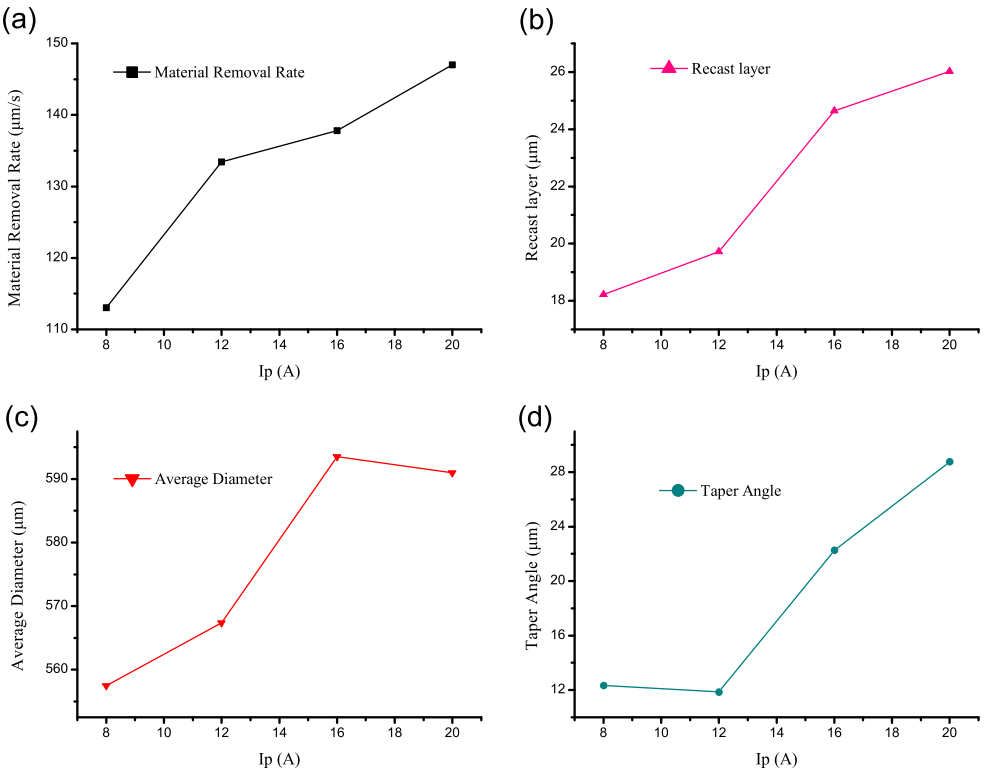

Fig. 4 **a**–**d** Effects of peak current on machining performance

all these factors, the ideal value of the peak current is found to be 12 A. Figure 5 shows entrance-side scanning electron microscope (SEM) images of micro-holes for different peak currents.

3.1.2 Effects of pulse duration on machining performance

Figure 6 shows the effects of pulse duration T_{on} on machining performance in terms of MRR, thickness of recast layer, average

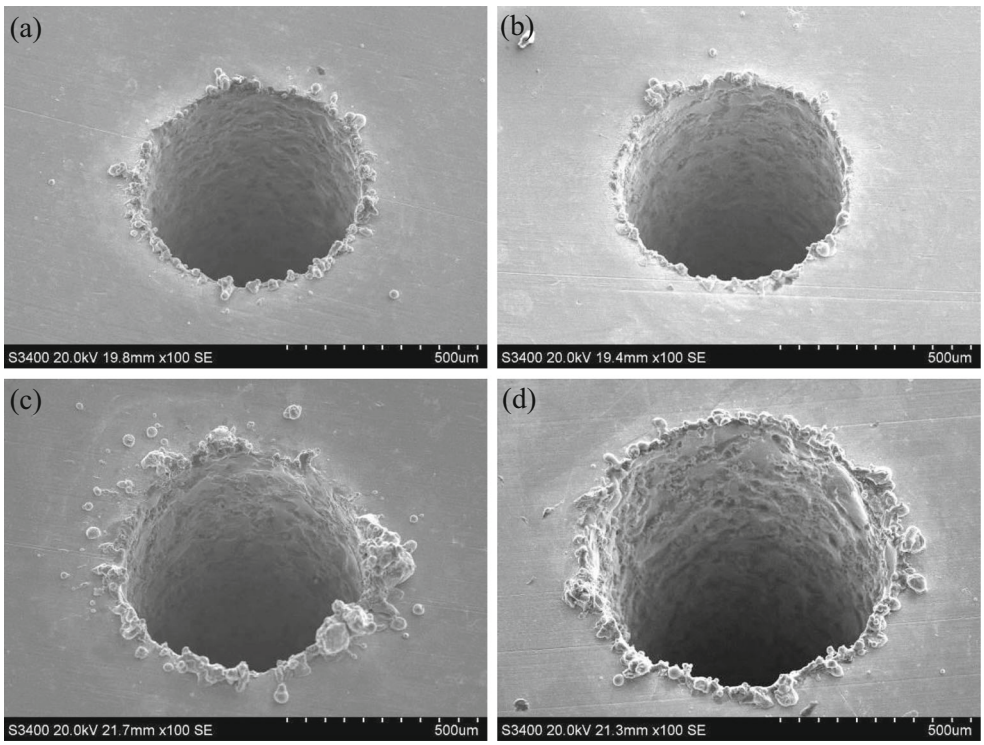

Fig. 5 SEM images of holes machined with different values of peak current: **a** 8 A, **b** 12 A, **c** 16 A, **d** 20 A

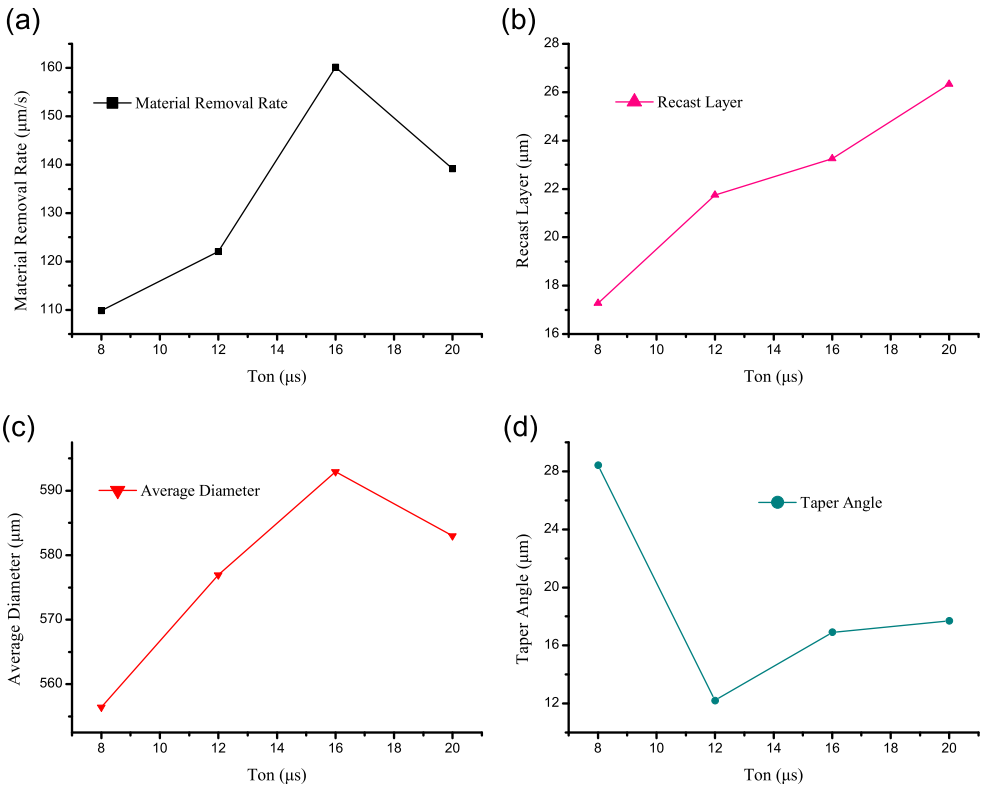

Fig. 6 **a**–**d** Effects of pulse duration on machining performance

diameter, and taper angle. The other machining parameters are set at a peak current of 12 A and pulse interval of 24 μs. It can be seen from Fig. 6a that there is an upward trend in MRR until T_{on}=16 μs, after which it falls sharply. The average diameter, plotted in Fig. 6c, shows a similar trend. This is because the pulse on-time is the effective machining time in each pulse cycle, and so an increase in pulse duration will inevitably increase the MRR and average diameter. However, a longer pulse duration can

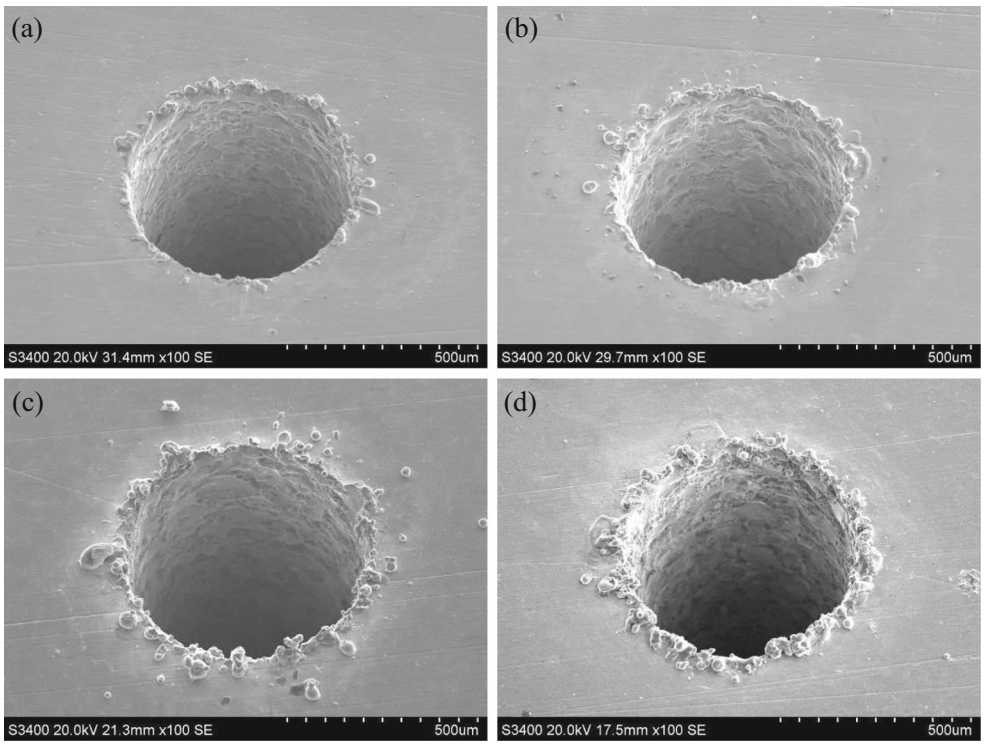

Fig. 7 SEM images of holes machined with different values of the pulse duration: **a** 8 μs, **b** 12 μs, **c** 16 μs, **d** 20 μs

result in arcing and machining instability. Thus, the removal rates in the frontal and lateral gaps decrease. Therefore, a long pulse on-time is not appropriate for good performance of EDM. The thickness of the recast layer steadily increases with increasing T_{on}, as shown in Fig. 6b. This is due to the fact that for each spark, a longer pulse duration supplies more energy, which results in a broader and deeper recast layer. At the same time, with increasing pulse duration, the taper angle falls to a minimum value and then increases steadily. Hence, there should be a suitable value of T_{on} that gives a high MRR, small diameter and taper angle, and a thin recast layer. It turns out that to obtain the best performance, T_{on} should be set at 12 μs. Figure 7 shows entrance-side SEM images of micro-holes for different pulse durations.

3.1.3 Effects of pulse interval on machining performance

Figure 8 shows the relationship between pulse interval T_{off} and machining performance. The other machining parameters are set at a peak current of 12 A and pulse duration of 12 μs. It is found that MRR, thickness of recast layer, average diameter, and taper angle decrease almost linearly with increasing T_{off}. The pulse interval can be considered as the period where machining halts for deionization. With increasing pulse interval, expansion of the frontal and lateral gaps will slow, resulting in a lower MRR and a smaller average diameter. Moreover, it is found that the recast layer thickness and the taper angle tend to decrease with increasing T_{off}. Thus, to achieve higher machining efficiency, T_{off} should be set at a lower value. In contrast, to improve dimensional accuracy, a higher T_{off} is appropriate. Therefore, an ideal pulse interval should be chosen that will provide both a high MRR and good machining quality, and it turns out that a value of 36 μs is appropriate. Figure 9 shows entrance-side images of micro-holes for different pulse intervals.

Overall, the better machining performance can be obtained with a combination of a 12-μs pulse duration, a 36-μs pulse interval, and a 12-A peak current, which gives a moderately high MRR, good dimensional accuracy, and a thin recast layer. The dimensional accuracy and high surface quality can be seen in Fig. 10, with a hole diameter of 573.418 μm, and the thin recast layer (less than 20 μm) can be seen in Fig. 11.

3.2 ECM process

3.2.1 Impacts of machining time and voltage on machining gap

The machining gap formed after EDM is employed as the initial gap in the ECM process. The flushing pattern is changed to lateral, with the salt solution being supplied to the machining gap. The effects of different machining times and voltages on expansion of the radial gap are shown in Fig. 12. It is found that at the same machining voltage, a longer machining time will result in a bigger radial gap. This is because a longer machining time allows material dissolution to occur to a greater extent, resulting in a larger-diameter micro-hole.

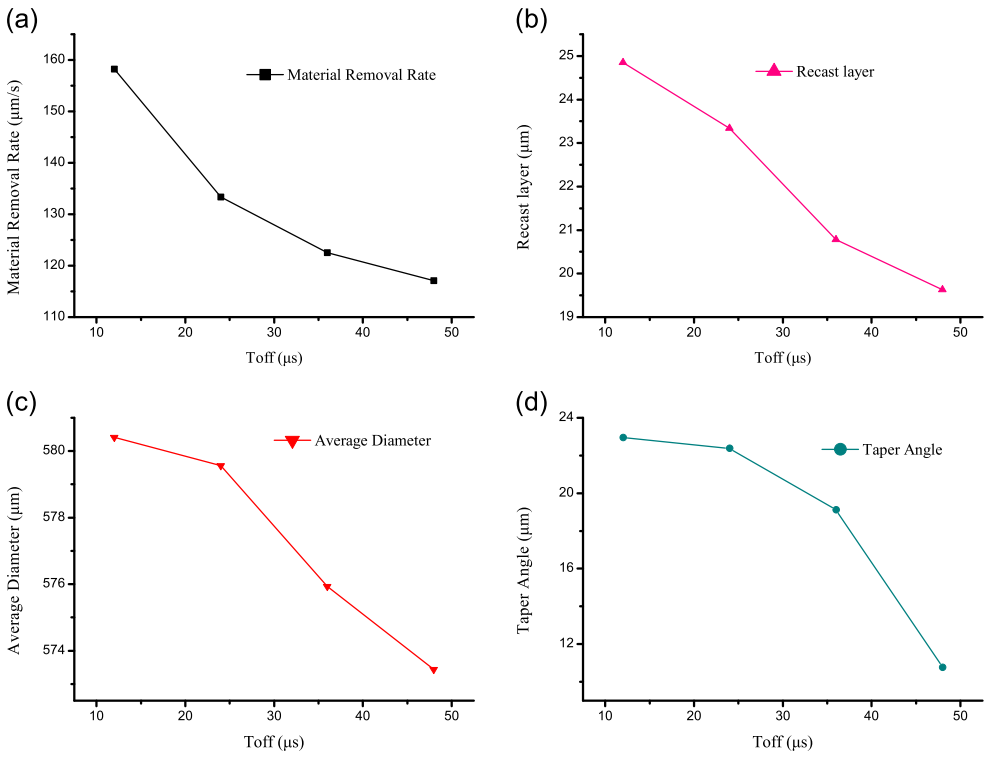

Fig. 8 **a**–**d** Effects of pulse interval on machining performance

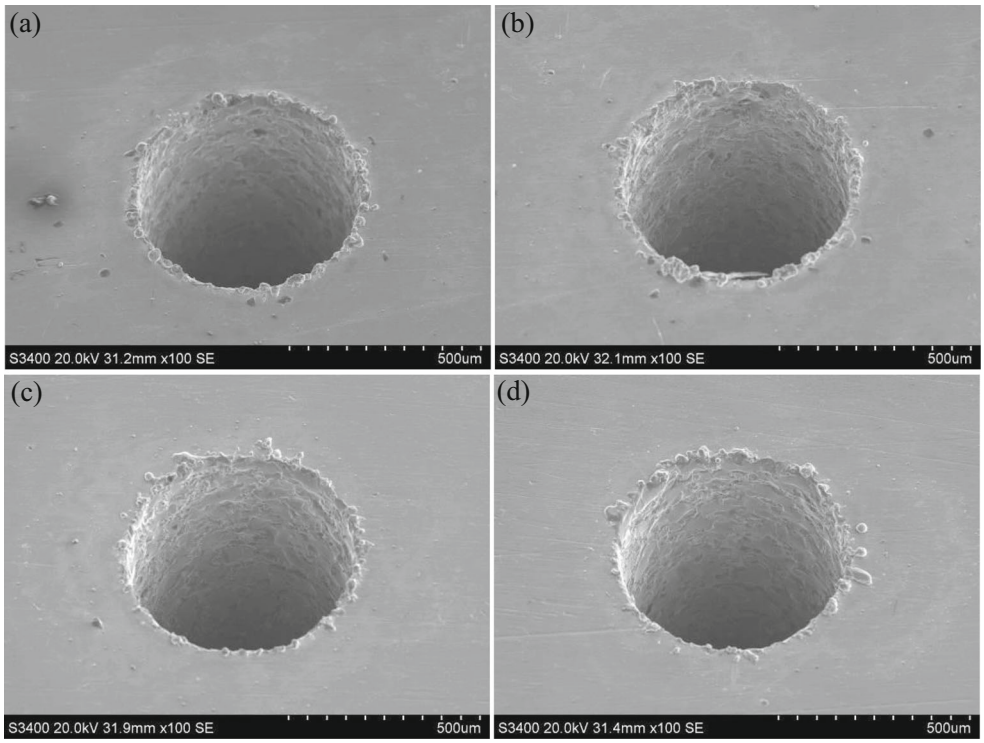

Fig. 9 SEM images of holes machined with different values of the pulse interval: **a** 12 μs, **b** 24 μs, **c** 36 μs, **d** 48 μs

It is also found that for a fixed machining time, a higher machining voltage will result in expansion of the radial gap. Furthermore, at longer machining times, the trend of expansion is more obvious. The largest radial gap is found to be 180.284 μm at 45 V and 60 s. This behavior results from the fact that for the same duration, a higher voltage supplies more energy to dissolve anode material.

Holes machined using different machining parameters are shown in Fig. 13. The pure EDM process, in which the parameters are set at a combination of a 12-μs pulse duration, a 36-μs pulse interval, and a 12-A peak current, is compared with the EDM and ECM combined process. Figure 13a shows the result of pure EDM, for which the hole diameter is 573.418 μm and for which the hole wall is covered with overlapping discharge craters, producing a rough surface. When ECM is subsequently carried out to dissolve the surface produced by EDM, the radial gap enlarges further. The better-machined results for three different voltages are shown in Fig. 8b–d, respectively. As shown in Fig. 8b, for 15 V/30 s, the radial gap is slightly expanded, although the machined surface is still rough. This can be explained by the fact that the thickness of the material layer that the electrochemical reaction would be able to dissolve is smaller than the roughness of the surface machined by EDM. Therefore, it is difficult to obtain a hole with better surface quality at a voltage as

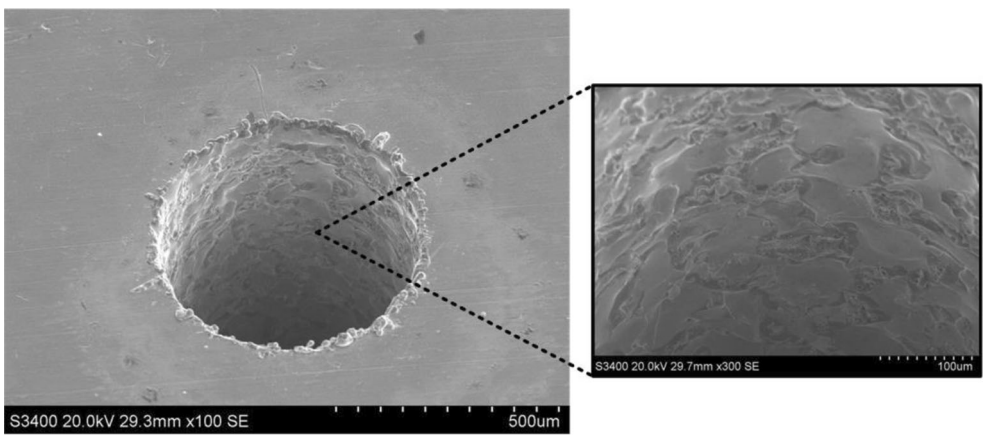

Fig. 10 SEM image of entrance and lateral wall

low as 5 V. For machining voltages of 30 and 40 V, the radial gap is expanded to 130 and 215 μm, respectively, and the smoothness of the machined surface is clearly improved.

In addition, there exist some limitations in the application for this method. To be exact, there are some obstacles in machining the holes with micro-diameter. Especially for the hole diameter smaller than 500 μm, it is difficult to guarantee the stability of flushing in ECM process, due to the narrow lateral machining gap. Besides, the tubular electrode with small diameter is very soft and pliable. When the side flushing is employed in the ECM process, the tubular electrode could likely be diverted from rotating center and then touch the machined surface in the narrow gap, which will result in the short circuit and secondary discharge and affect the surface quality.

3.2.2 Improvements in surface quality

Figure 14 compares surfaces machined by EDM alone and by the EDM/ECM in situ combined process. It can be seen from Fig. 14a that for EDM alone, the machined surface is entirely covered with a re-solidified layer. It is clear from the magnified image that this layer contains cracks, as well as voids and metal globules. It is clear from Fig. 14b that when the surface produced by EDM is further machined by ECM, the surface roughness is remarkably improved and the whole machined area also becomes smoother. It can be seen from the magnified image that surface defects such as cracks, voids, and metal globules are swept away. This illustrates how the electrochemical reaction occurring on the surface results in material removal by ion dissolution, thereby causing the surface defects due to EDM to disappear and producing a better surface finish. It demonstrates that the tubular electrode EDM/ECM in situ combined process is effective in obtaining a smooth surface.

The improvement in surface quality can also be seen from Fig. 15, which shows a comparison of three-dimensional topographies for surfaces machined by EDM alone and by EDM plus ECM. Observation of the initially machined surface in Fig. 15a reveals that it consists of many humps and craters and has a high surface roughness. However, after ECM, the surface is significantly improved, as shown in Fig. 15b. The machined surface is now smooth and regular. This again illustrates that after ECM, the surface defects generated by EDM are entirely dissolved. Finally, the surface is finished and free of recast layer.

3.2.3 Removal of recast layer

The recast layer was examined metallographically. After cutting, polishing, and etching, cross sections of the recast layer were analyzed under a metallographic microscope. The results of combined EDM plus ECM are compared with those of EDM alone in Fig. 16. It can be seen that after the initial

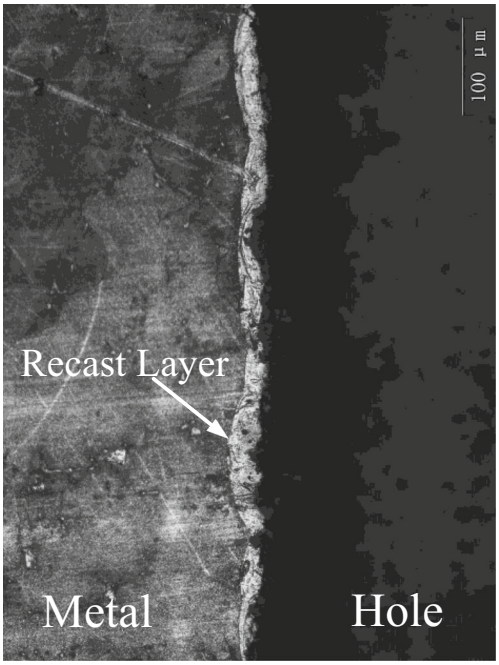

Fig. 11 Metallographic microscope image of recast layer

EDM, the machined surface is entirely covered by a recast layer that includes many cracks and voids, whereas after further ECM, the recast layer has completely vanished. This is in accord with the previous results on surface quality. After the EDM drilling, the ECM expands the hole in the radial direction, whereby the recast layer generated by EDM is removed and the surface becomes smoother. Hence, these results confirm that the EDM/ECM in situ combined process is effective in producing film cooling holes without a recast layer.

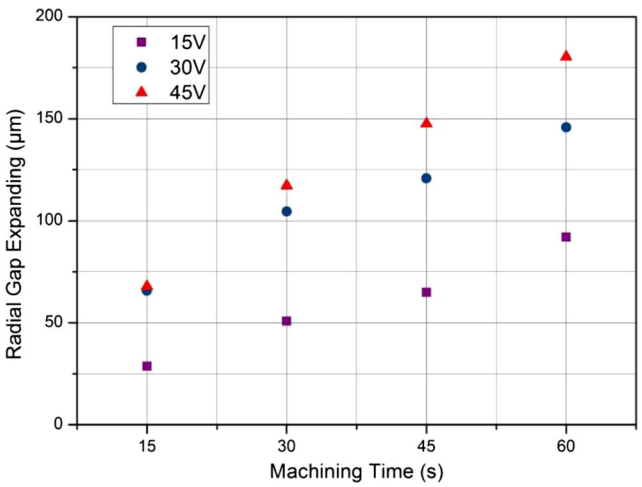

Fig. 12 Expansion of the radial gap for different machining times and voltages

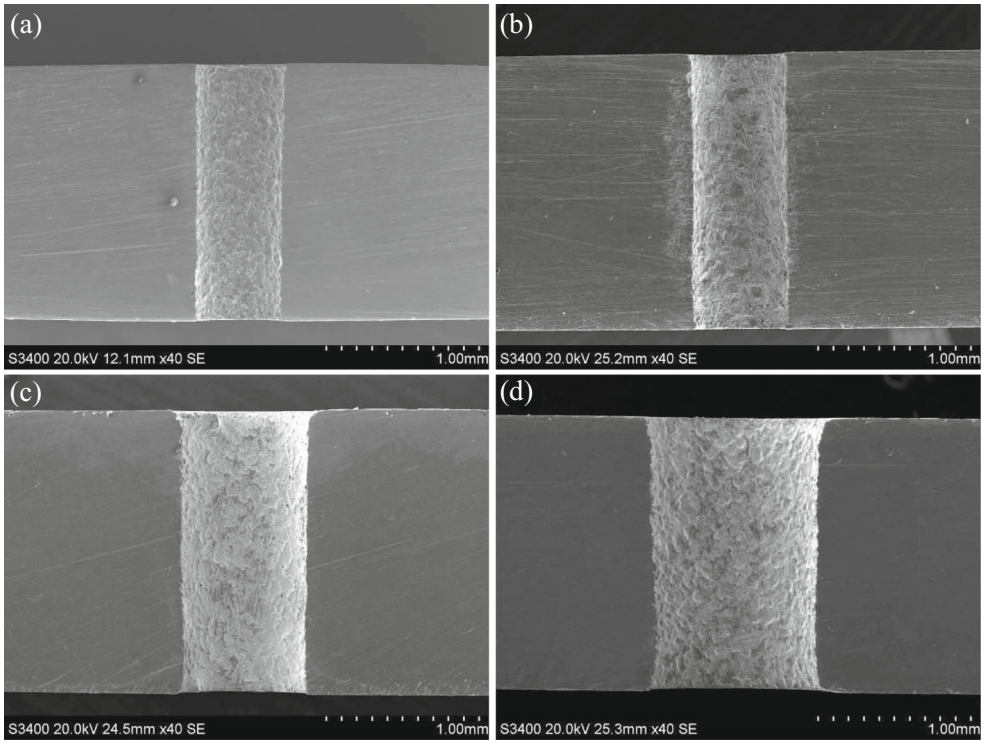

Fig. 13 SEM cross-sectional images for different machining conditions: **a** EDM alone; **b** 15 V, 30 s; **c** 30 V, 30 s; **d** 45 V, 45 s

4 Conclusions

In this paper, a tubular electrode electro-discharge high-speed drilling/ECM in situ combined process has been presented. A tubular electrode and a specially designed flushing device are used, with internal and side flushing being performed at the same time so that tubular electrode electro-discharge high-speed drilling and ECM can

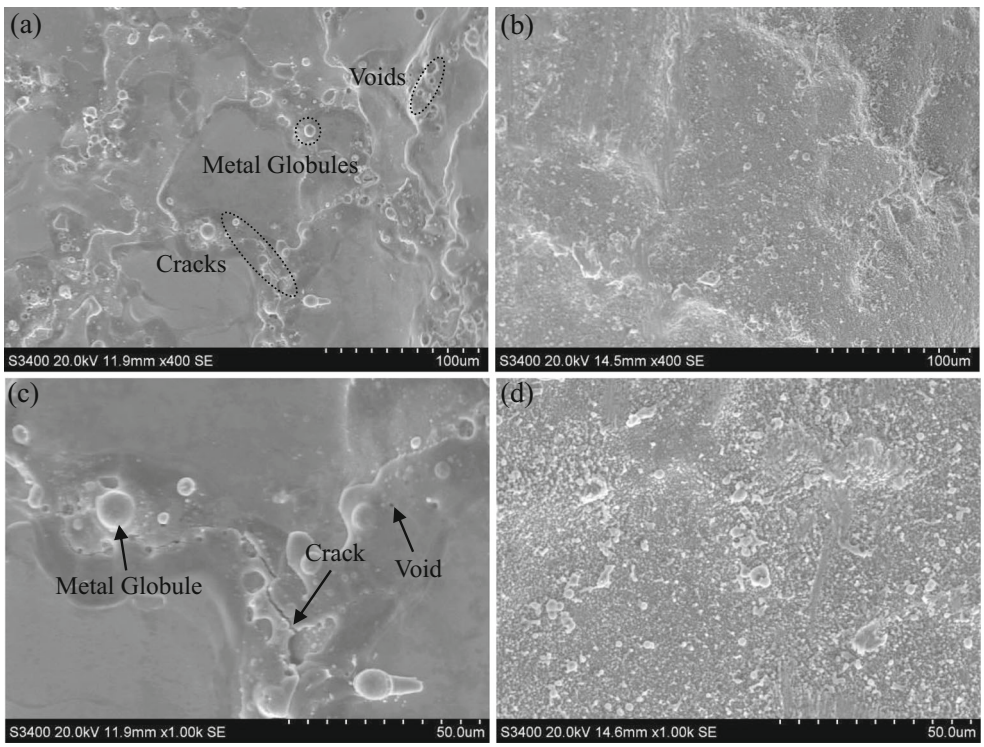

Fig. 14 Comparison of machined surfaces: **a** after EDM; **b** after further ECM; **c**, **d** Magnified views of portions of (**a**) and (**b**), respectively

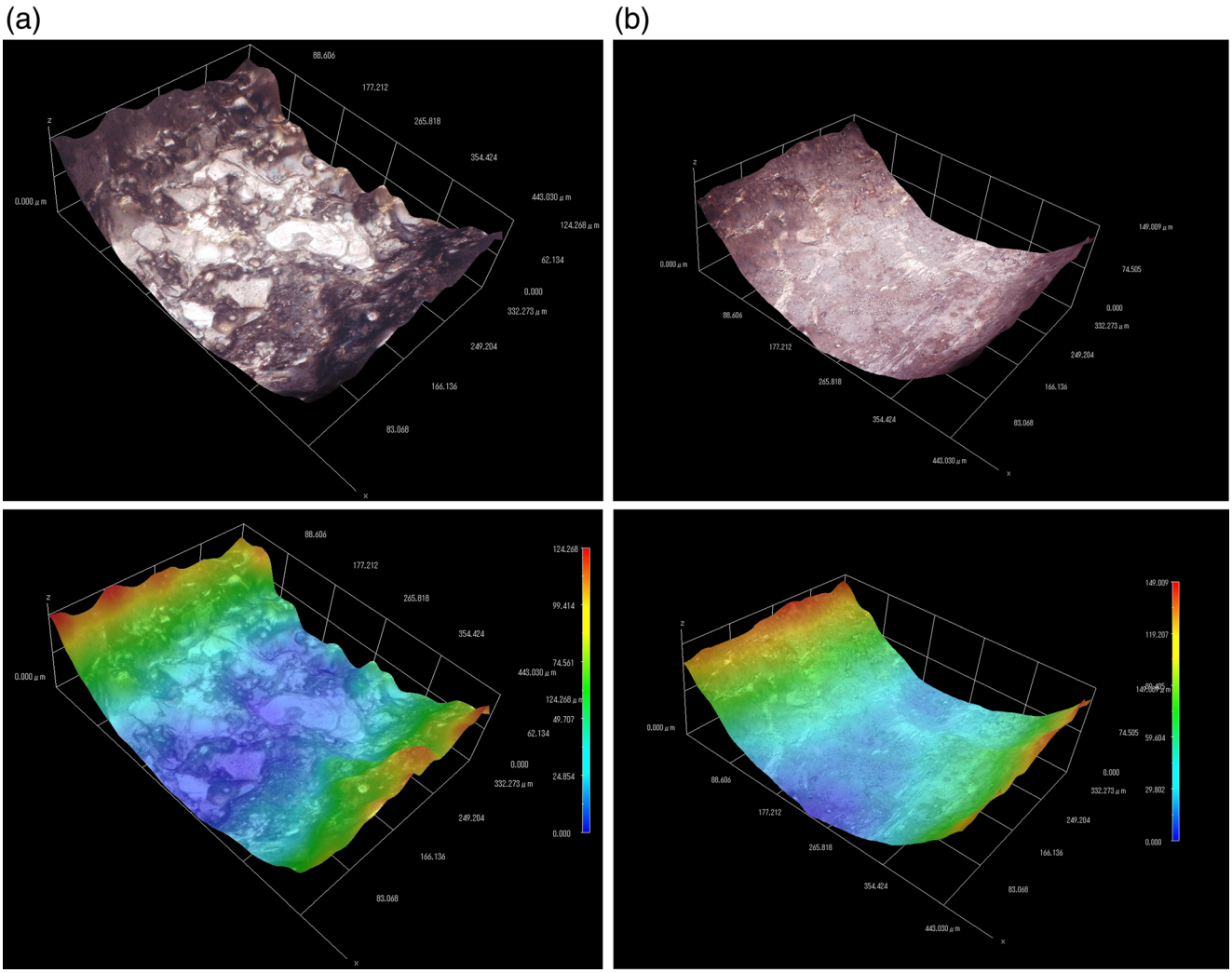

Fig. 15 Micrographs and three-dimensional topographies of hole surfaces: **a** after EDM, **b** after EDM + ECM

be combined in situ. The performance of the technique has been investigated on a nickel-based superalloy. The following conclusions can be drawn:

1. The experimental investigations of the effects of different parameters of the EDM process on machining performance show that to achieve the best performance, the

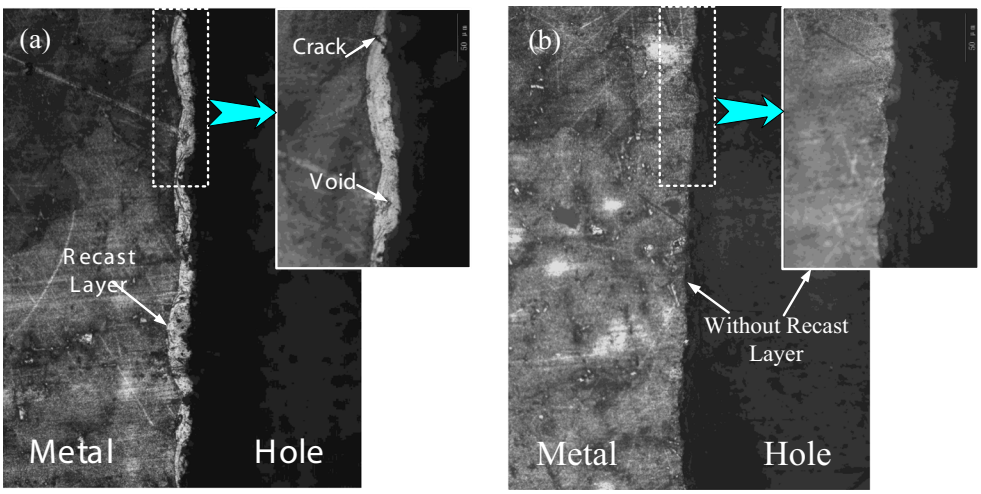

Fig. 16 Metallographic microscope images of cross sections machined by different processes: **a** EDM alone, **b** EDM + ECM

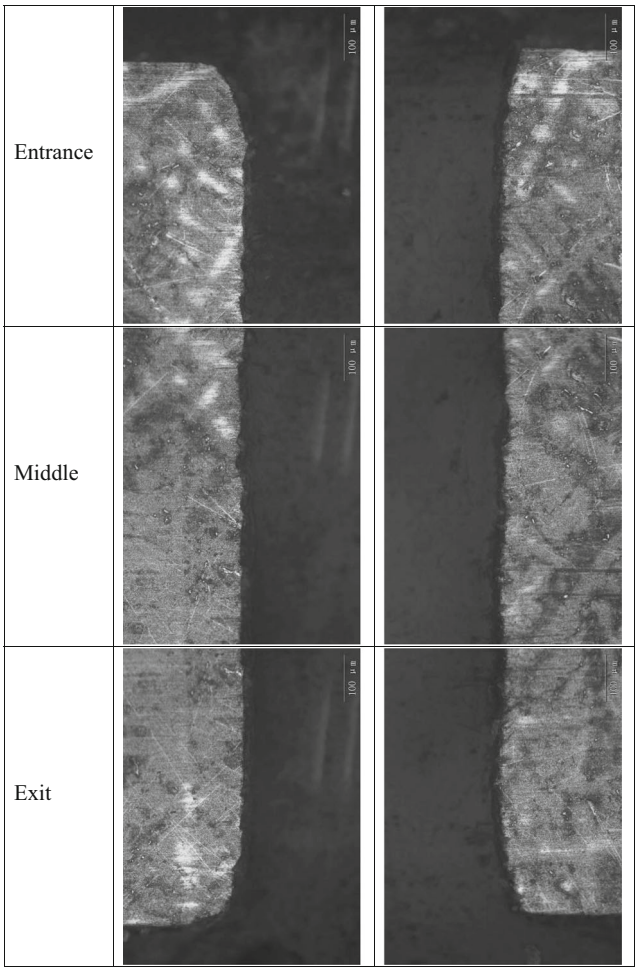

Fig. 17 Hole machined by the EDM/ECM in situ combined process without a recast layer

ideal values of peak current, pulse duration, and pulse interval are 12 A, 12 μs, and 36 μs, respectively.

2. The experimental results show that ECM could be employed to remove the rough surface produced by EDM. It is found that the EDM/ECM in situ combined process improves the surface quality compared with that produced by EDM alone and removes the recast layer generated by the latter.
3. It has been shown that the EDM/ECM in situ combined process is a viable approach for the production of film cooling holes, especially with diameters greater than 0.5 mm, without a recast layer. As shown in Fig. 17, the cross sections of the entire hole were investigated by metallographic microscopic analysis. The hole was divided into six parts, with each part being examined independently. It can be seen that the recast layer is completely removed from the hole by electrochemical dissolution. This provides further confirmation that film cooling holes without a recast layer can be drilled by the EDM/ECM in situ combined process.

Acknowledgments The authors acknowledge financial support provided by the China Natural Science Foundation (51475237), the National High-Tech Research and Development Program of China (2013AA040101), the Program for New Century Excellent Talents in University (NCET-12-0627), and the Funding of Jiangsu Innovation Program for Graduate Education (KYLX_0232).

Compliance with ethical standards No human participants or animals are involved in the research. The manuscript has not been published previously (partly or in full) and has not been submitted to more than one journal for simultaneous consideration. No data have been fabricated or manipulated (including images) to support our conclusions.

Conflict of interest The authors declare that they have no competing interests.

References

1. Bilgi DS, Jain VK, Shekhar R, Mehrotra S (2004) Electrochemical deep hole drilling in super alloy for turbine application. J Mater Process Technol 149(1–3):445–452
2. Liu K, Yang SF, Han JC (2014) Influence of coolant density on turbine blade film-cooling with axial and compound shaped holes. J Heat Trans-T ASME 136(4):1–5
3. Fang XL, Qu NS, Li HS, Zhu D (2013) Enhancement of insulation coating durability in electrochemical drilling. Int J Adv Manuf Technol 68(9–12):2005–2013
4. Ferraris E, Castiglioni V, Ceyssens F, Annoni M, Lauwers B, Reynaerts D (2013) EDM drilling of ultra-high aspect ratio micro holes with insulated tools. Ann CIRP 62(1):191–194
5. Liu K, Lauwers B, Reynaerts D (2010) Process capabilities of micro-EDM and its applications. Int J Adv Manuf Technol 47(1–4):11–19
6. Li JZ, Shen FH, Yu ZY, Natsu W (2013) Influence of microstructure of alloy on the machining performance of micro EDM. Surf Coat Tech 228(1):460–465
7. Nikalje AM, Kumar A, Srinadh KVS (2013) Influence of parameters and optimization of EDM performance measures on MDN 300 steel using Taguchi method. Int J Adv Manuf Technol 69(1–4):41–49
8. D'Urso G, Maccarini G, Ravasio C (2014) Process performance of micro-EDM drilling of stainless steel. Int J Adv Manuf Technol 72(9–12):1287–1298
9. Hao Ning C, Wang JJJ (2011) An analysis of overcut variation and coupling effects of dimensional variable in EDM process. Int J Adv Manuf Technol 55(9–12):935–943
10. Nguyen MD, Rahman M, San Wong Y (2012) An experimental study on micro-EDM in low-resistivity deionized water using short voltage pulses. Int J Adv Manuf Technol 58(5–8):533–544
11. Wang CC, Chow HM, Yang LD, Lu CT (2009) Recast layer removal after electrical discharge machining via Taguchi analysis: a feasibility study. J Mater Process Technol 209(8):4134–4140
12. Amineh SK, Tehrani AF, Mohammadi A (2013) Improving the surface quality in wire electrical discharge machined specimens by removing the recast layer using magnetic abrasive finishing method. Int J Adv Manuf Technol 66(9–12):1793–1803
13. Cusanelli G, Hessler-Wyser A, Bobard F, Demellayer R, Perez R, Flükiger R (2004) Microstructure at submicron scale of the white layer produced by EDM technique. J Mater Process Technol 149(1):289–295
14. Lee HT, Tai TY (2003) Relationship between EDM parameters and surface crack formation. J Mater Process Technol 142(3):676–683
15. McGeough JA, Khayry ABM, Munro W, Crookall JR (1983) Theoretical and experimental investigation of the relative effects

of spark erosion and electrochemical dissolution in electrochemical arc machining. Ann CIRP 32(1):113–118
16. Kurita T, Hattori M (2006) A study of EDM and ECM/ECM-lapping complex machining technology. Int J Mach Tool Manuf 46(14):1804–1810
17. Chung DK, Shin HS, Kim BH, Park MS, Chu CN (2009) Surface finishing of micro-EDM holes using deionized water. J Micromech Microeng 19(4):1–7
18. Ramasawmy H, Blunt L, Rajurkar K (2005) Investigation of the relationship between the white layer thickness and 3D surface texture parameters in the die sinking EDM process. Precis Eng 29(4): 479–490
19. Zeng Z, Wang Y, Wang Z, Shan D, He X (2012) A study of micro-EDM and micro-ECM combined milling for 3D metallic microstructures. Precis Eng 36(3):500–509
20. Klocke F, Klink A, Veselovac D, Aspinwall DK, Soo SL, Schmidt M, Schilp J, Levy G, Kruth J-P (2014) Turbomachinery component manufacture by application of electrochemical, electro-physical and photonic processes. Ann CIRP 63(2):703–726
21. Thanigaivelan R, Arunachalam RM, Drukpa P (2012) Drilling of micro-holes on copper using electrochemical micromachining. Int J Adv Manuf Technol 61(9–12):1185–1190
22. Zhu D, Wang W, Fang X, Qu N, Xu Z (2010) Electrochemical drilling of multiple holes with electrolyte-extraction. Ann CIRP 59(1):239–242
23. Ramasawmy H, Blunt L (2007) Investigation of the effect of electrochemical polishing on EDM surfaces. Int J Adv Manuf Technol 31(11–12):1135–1147
24. Lauwers B, Klocke F, Klink A, Tekkaya AE, Neugebauer R, McIntosh D (2014) Hybrid processes in manufacturing. Ann CIRP 63(2):561–583
25. Skoczypiec S, Ruszaj A (2014) A sequential electrochemical-electrodischarge process for micropart manufacturing. Precis Eng 38(3):680–690
26. Nguyen MD, Rahman M, Wong YS (2012) Simultaneous micro-EDM and micro-ECM in low-resistivity deionized water. Int J Mach Tool Manuf 54:55–65